

# Metal Sintering in Rh/Al<sub>2</sub>O<sub>3</sub> Catalysts Followed by HREM, <sup>1</sup>H NMR, and H<sub>2</sub> Chemisorption

C. Force,<sup>\*,†</sup> A. Ruiz Paniego,<sup>‡</sup> J. M. Guil,<sup>‡</sup> J. M. Gatica,<sup>§</sup> C. López-Cartes,<sup>§</sup> S. Bernal,<sup>§</sup> and J. Sanz<sup>†</sup>

*Instituto de Ciencia de Materiales de Madrid, CSIC; Campus Universitario de Cantoblanco, 28049 Madrid, Spain, Instituto de Química Física "Rocasolano", CSIC, Serrano 119, 28006 Madrid, Spain, and Facultad de Ciencias, Universidad de Cádiz, Apartado 40, Puerto Real 11510, Cádiz, Spain*

Received September 8, 2000. In Final Form: January 31, 2001

Hydrogen adsorption on Rh/Al<sub>2</sub>O<sub>3</sub> catalysts sintered at increasing temperatures has been analyzed with high-resolution electron microscopy (HREM), proton nuclear magnetic resonance (<sup>1</sup>H NMR), and microcalorimetric techniques. The <sup>1</sup>H NMR technique has been used to differentiate hydrogen adsorption on metal particles from that produced on the support. Metal dispersions estimated by HREM are intermediate between those deduced from volumetry and NMR techniques. Metal particle sizes deduced from HREM histograms, once weighted for surface effects, agree well with those determined by NMR but differ appreciably from those calculated from volumetric data. Observed differences have been ascribed to hydrogen retained on Al<sub>2</sub>O<sub>3</sub> near Rh particles, that increases the NMR line located at the resonance frequency. The dependence of the NMR shift associated with hydrogen adsorbed on the rhodium is discussed in terms of metal particle size. In samples with low metal loadings, a partial coverage of metal particles with Al<sub>2</sub>O<sub>3</sub> moieties, deposited during catalyst preparation, has been detected that reduces observed <sup>1</sup>H NMR shifts.

## Introduction

Petrochemical industries rely on metal catalysts for the manufacture of a wide range of products. For optimal use of supported metal catalysts, the  $\gamma$ -Al<sub>2</sub>O<sub>3</sub> support is extensively used because of its high surface area and thermal stability. Metal particles formed during reduction of metal precursors are usually characterized by H<sub>2</sub> and O<sub>2</sub> chemisorption, giving information about metal dispersions, that is, the relative number of metal atoms placed at the metal particle surface susceptible to participate in catalytic reactions. However, the presence of spill-over phenomena and metal-support interactions make metal dispersion determinations by selective chemisorption difficult.<sup>1-3</sup> At this point, the <sup>1</sup>H NMR technique, capable of differentiating hydrogen adsorbed on the metal from that adsorbed on the support, is extremely useful as shown elsewhere by several groups.<sup>1,4,5</sup> Moreover, the position of the shifted NMR line, associated with hydrogen adsorbed on the metal, varies with the metal particle size. From this fact, this parameter could be also used to characterize metal particles formed. However, metal deactivation produced by metal poisoning or metal-support interactions could significantly affect this parameter.<sup>6,7</sup>

In this work, hydrogen adsorption on Rh/Al<sub>2</sub>O<sub>3</sub> catalysts has been studied by H<sub>2</sub> chemisorption and <sup>1</sup>H NMR techniques, and metal dispersions so determined are compared with those deduced by the high-resolution electron microscopy (HREM) technique. This study has been carried out in two Rh/Al<sub>2</sub>O<sub>3</sub> catalysts with different metal loadings, submitted to increasing sintering temperatures. Finally, the dependence of NMR shifts with metal particle size has been compared with that of differential adsorption heats measured by microcalorimetry.

## Experimental Method

**Samples.** A  $\gamma$ -Al<sub>2</sub>O<sub>3</sub> sample, Girdler T-126, with a purity of 99.9% ( $S_{\text{BET}} = 149 \text{ m}^2 \text{ g}^{-1}$ , pore volume =  $0.56 \text{ cm}^3 \text{ g}^{-1}$ , mean pore diameter = 7.5 nm), was used to prepare Rh/Al<sub>2</sub>O<sub>3</sub> samples. Catalyst precursors were prepared by the incipient wetness impregnation method with solutions of Rh(NO<sub>3</sub>)<sub>3</sub>, chosen to give final metal loadings of 0.5% and 2% (samples M05 and M2). After impregnation, M05 and M2 samples were maintained at 373 K overnight and reduced under H<sub>2</sub> flow, at 673 K. Sintering of the catalysts was produced by cumulative thermal treatments, and samples were labeled with the temperature of sintering, so they are named M2 for the nonsintered sample and M2-917 K and M2-988 K for samples sintered at the two indicated temperatures. The M05, M05-962 K, and M05-988 K samples were labeled in the same way.

Prior to NMR, volumetric, and calorimetric experiments, the samples were submitted to a standard treatment consisting of oxidation at 473 K, reduction at 673 K, and outgassing at 473 K. After this treatment, H<sub>2</sub> adsorption was performed at 298 K at increasing pressures. Samples were thermally treated in Pyrex tubular cells provided with high-vacuum stopcocks.

**Techniques.** A heat flow microcalorimeter of the Tian-Calvet type was used to determine differential adsorption heats as a function of hydrogen uptake.<sup>8,9</sup> Previous treatment of catalysts was carried out in the calorimeter cell at 673 K.<sup>10</sup> The limit of detection of the calorimeter is 0.2 mJ or 2  $\mu$ W, and the

\* To whom correspondence should be addressed. E-mail: Cforce@icmm.csic.es. Fax: +34 91 3720623. Tel: +34 91 334 90 00, ext 266.

<sup>†</sup> Instituto de Ciencia de Materiales de Madrid, CSIC.

<sup>‡</sup> Instituto de Química Física "Rocasolano", CSIC.

<sup>§</sup> Facultad de Ciencias, Universidad de Cádiz.

(1) Rouabah, D.; Benslama, R.; Fraissard, J. J. *Chem. Phys. Lett.* **1991**, *179* (3), 218-222.

(2) Sheng, T.-C.; Gay, I. J. *Catal.* **1982**, *77*, 53-56.

(3) Chesters, A. M.; Packer, K.; Viner, H.; Wright, A. J. *Chem. Soc., Faraday Trans.* **1995**, *91*, 2203.

(4) Belzunegui, J. P.; Rojo, J. M.; Sanz, J. J. *Chem. Soc., Faraday Trans.* **1989**, *85*, 4287-4293.

(5) (a) Wu, X.; Gerstein, B. C.; King, T. S. *J. Catal.* **1989**, *118*, 238-254. (b) King, T. S.; Wu, X.; Gerstein, B. C. *J. Am. Chem. Soc.* **1986**, *108*, 6056-6058.

(6) Huges, R. In *Deactivation of Catalysts*; Academic: New York, 1984; Chapter 4.

(7) Butt, J. B.; Peterson, E. E. *Activation, Deactivation and Poisoning of Catalysts*; Academic: New York, 1988; Chapter 15.

(8) Herrmann, J. M. *J. Catal.* **1989**, *118*, 43-53.

(9) Trejo-Menayo, J. M. Doctoral Thesis, Madrid, 1990.

reproducibility on amounts adsorbed is better than 0.2  $\mu\text{mol}$ . The heat/voltage proportionality constant of the microcalorimeter was determined by the Joule effect. Corrections associated with the gas compression were determined from helium expansions to obtain isosteric heats of adsorption.

The Fourier transform infrared (FTIR) spectra were recorded on a Mattson instrument, model 5020; 250 scans at 4  $\text{cm}^{-1}$  resolution being routinely averaged. Acquisition and processing of the spectrometer signal were performed by using the FIRST software package. With the help of a conventional high-vacuum quartz cell, a self-supported disk (13 mg of sample per  $\text{cm}^2$ ) of the Rh/Al<sub>2</sub>O<sub>3</sub> catalyst was reduced in situ with flowing H<sub>2</sub> for 1 h at 723 K, then evacuated at 723 K for 1 h, and finally cooled to 298 K under vacuum. The spectrum recorded for this sample was used as a reference. The reduced/evacuated catalyst sample was further put in contact with 40 Torr of D<sub>2</sub>, at 298 K, and the evolution with time of its spectrum in the O–D stretching region was studied.

<sup>1</sup>H NMR spectra were obtained in special cells, directly connected to the volumetric apparatus, to correlate spectral modifications to the amount of H<sub>2</sub> adsorbed. NMR spectra were recorded at room temperature with a SXP 4/100 spectrometer equipped with an Aspect 2000 Fourier transform unit. The NMR frequency used was 67 MHz. The spectra were taken after  $\pi/2$  pulse excitations (3.5  $\mu\text{s}$ ), and the interval between successive accumulations (1 s) was chosen to avoid saturation effects. The number of accumulations (300–500) was selected to maintain an appropriate signal-to-noise ratio ( $S/N = 20$ ). Intensities of the NMR lines were determined by comparing the integrated intensities with that of a known external mica specimen.

The HREM micrographs were obtained with a JEOL-2000EX transmission electron microscope with 2.1 Å point resolution. The experimental images were digitized on a high-resolution CCD camera, COHU-4910, using the SEMPER 6+ software.<sup>11</sup> Particle size distribution curves were calculated from the measurement of a significant number of Rh metal particles. Mean particle size, mass-corrected mean particle size, and metal dispersion  $R_h_s/R_h_T$  (where  $R_h_s$  and  $R_h_T$  stand for surface and total numbers of rhodium atoms, respectively) were calculated according to the methodology described elsewhere.<sup>12</sup>

## Results

**Volumetric and Calorimetric Data.** All isotherms are of the Langmuir type, Figure 1. They display a significant adsorption of hydrogen at low pressure, a knee at  $\approx 5$  Torr, and a smooth linear increase in their final part. After sample outgassing at room temperature, the hydrogen desorbed can be reversibly readsorbed in a second adsorption experiment. The difference between the two isotherms gives the amount of hydrogen strongly adsorbed on the catalyst (arrows in Figure 1).

The amount of hydrogen adsorbed on the metal increases as metal particle size decreases. Metal dispersion can be directly estimated if adsorption takes place only on the metal particles and the H/Rh stoichiometry of 1:1 is obeyed. In both sets of catalysts, metal dispersions, determined by extrapolation at low pressures of the linear part of the isotherm, decrease as the temperature of sintering increases (Table 1).

Differential adsorption heats obtained in the catalysts as a function of hydrogen adsorption are shown in Figure 2. In all cases,  $q^{st,\sigma}$  progressively decreases as the amount of hydrogen adsorbed,  $n^\sigma$ , increases. All curves present two differentiated zones. In the case of the M2 sample, the adsorption heat ( $q^{st,\sigma}$ ) decreases from 50 to 35 kJ/mol in the first part of the curve (type I) and from 35 to 11

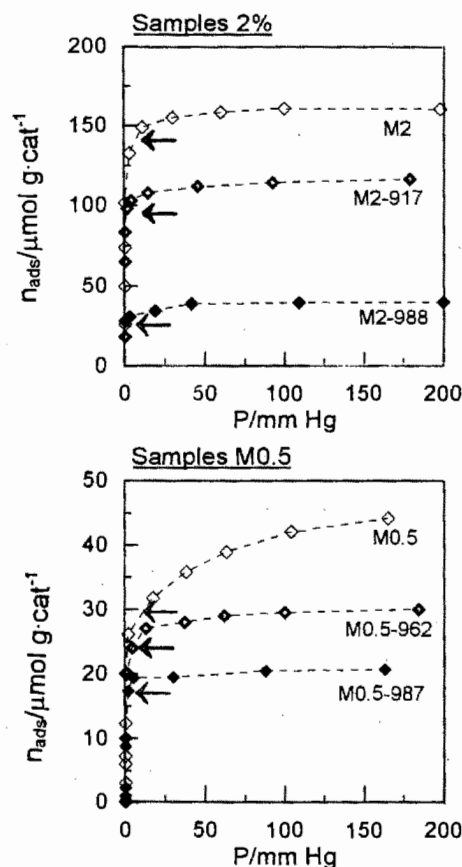


**Figure 1.** Hydrogen adsorption isotherms at 295 K on M05 and M2 samples. After the first adsorption experiments, the sample was outgassed at 298 K and a readsorption experiment was done. The difference between the two isotherms gives the amount of hydrogen strongly adsorbed on the metal (see arrows).

**Table 1.** Metal Dispersions Obtained with Volumetric, NMR, and HREM Techniques

sample	H/Rh ads vol	H/Rh NMR	Rhs/Rh HREM
M2	0.84	0.41	0.65
M2-917	0.67	0.28	0.41
M2-988	0.25	0.11	0.18
M05	1.10	0.53	0.69
M05-962	0.61	0.19	0.31
M05-988	0.50	0.16	0.28

kJ/mol in the second part of the curve (type II). Hydrogen readsorbed in samples outgassed at room temperature (not shown in Figure 2) reproduces the final part of the calorimetric curve. In the M2 catalyst sintered at 988 K, the  $q^{st,\sigma}$  initial value was around 42 kJ/mol and the amount of hydrogen of type II was lower. In the M05 sample, hydrogen adsorption shows a decrease of  $q^{st,\sigma}$  from 44 to 27 kJ/mol and then from 27 to 10 kJ/mol. In M05 catalysts sintered at 988 K, the amount of adsorbed hydrogen is lower, and the type I zone overlaps the corresponding region of the M05 curve. In the two catalysts sintered at the intermediate temperature, the curves run between those analyzed in Figure 2 (data not included).

**Nuclear Magnetic Resonance Data.** <sup>1</sup>H NMR spectra corresponding to H<sub>2</sub> adsorption on M2 and M05 catalysts are presented in Figure 3. The NMR spectra show two lines, one at the resonance frequency (line A) and other shifted upfield (line B). They have been previously assigned to OH groups of the support (line A) and hydrogen

(10) Guil, J. M.; Perez Masia, A.; Ruiz Paniago, A.; Trejo Menayo, J. M. *Thermochim. Acta* **1998**, *312*, 115–124.

(11) Bernal, S.; Botana, F. J.; Calvino, J. J.; Cifredo, G. A.; Perez Omil, J. A.; Pintado, J. M. *Catal. Today* **1995**, *28*, 219.

(12) Bernal, S.; Calvino, J. J.; Cauqui, M. A.; Pérez-Omil, J. A.; Pintado, J. M.; Rodríguez Izquierdo, J. M. *Appl. Catal., B* **1998**, *16*, 127–138.

(13) Sanz, J.; Rojo, J. M. *J. Phys. Chem.* **1985**, *89*, 4974.

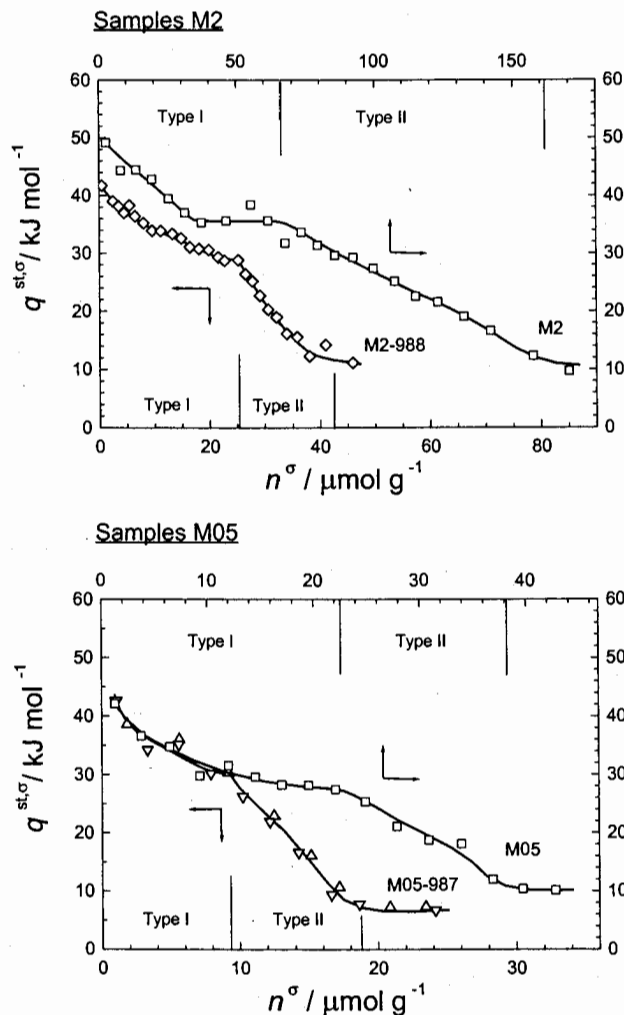
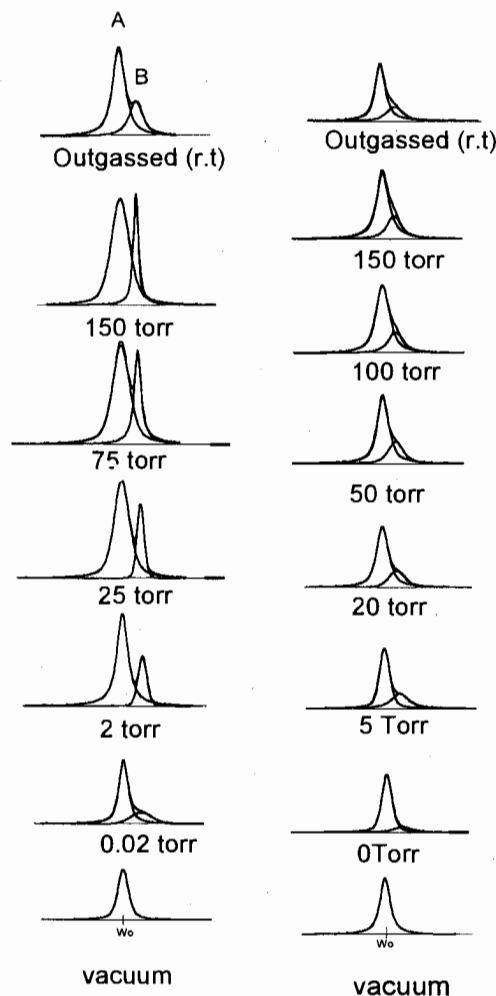


**Figure 2.** Evolution of differential adsorption heats ( $q^{\text{st},\sigma}$ ) in  $\text{kJ}(\text{mol H atoms})^{-1}$  versus hydrogen uptake,  $n^\sigma$  ( $\mu\text{mol g}^{-1}$ ), in fresh and 987–988 K sintered M05 and M2 catalysts.

adsorbed on metal particles (line B).<sup>13–15</sup> In M05 samples, the hydrogen adsorption does not considerably affect line A, but in sample M2 the intensity of this line increases appreciably with hydrogen adsorbed. In all cases, the shift of line B decreases as hydrogen adsorption progresses. Outgassing of the samples at room temperature decreases the intensity of line B and recovers shift values measured at low  $\text{H}_2$  coverage.

In all cases, plots of intensities Ia and Ib versus hydrogen pressure display characteristics of volumetric isotherms (Figure 4). In the case of the M2 catalyst, increments of line A are higher than those of line B; however, sintering of samples at increasing temperatures decreases the difference between Ia and Ib increments. In a similar way to that used in the analysis of the volumetric results, metal dispersions were determined from the intensity of line B. For this determination, intensities were calibrated with an external standard. Metal dispersions obtained by this method are considerably lower than those obtained with the volumetric technique (Table 1).

Variations on the position of the shifted line,  $\delta_B$ , versus intensity Ib are given in Figure 5. In general,  $\delta_B$  decreases slightly with the amount of hydrogen adsorbed on the



**Sample M2**

**Sample M05**

**Figure 3.** Deconvolution of  $^1\text{H}$  NMR spectra of hydrogen adsorption in M05 and M2 catalysts. The spectra of samples outgassed at room temperature after hydrogen adsorption are shown in the top of figure.

metal, up to pressures of 5 Torr, but decreases strongly at higher pressures. This fact has been previously ascribed to the existence of two types of sites with different chemical shifts on the metal.<sup>13</sup> Exchange of hydrogen between the two sites explains the presence of a single line, whose position and intensity depend on the relative amount of both species. Moreover, the observed variation of the chemical shift of line B requires that adsorption of hydrogen on the metal modifies the electronic interaction between the hydrogen and the metal.<sup>13</sup> The analysis of Figure 5 shows also that  $\delta_B$  values, measured at low pressures, decrease with metal sintering.

Other parameters considered in this work are the line width of line B and its dependence on the amount of hydrogen adsorbed on the metal. In all cases, line width decreases with the increase of hydrogen uptake (Figure 5). At low pressures, line widths remain almost constant, but at higher pressures they decrease as a consequence of hydrogen mobility. The decrease observed in the line width of component B corresponds to adsorption of hydrogen at the second type of sites of the metal. In all samples, the relative importance of the second part of these curves decreases with sintering treatments.

(14) Sanz, J.; Rojo, J. M.; Malet, P.; Munuera, G.; Blasco, M. T.; Conesa, J. C.; Soria, J. *J. Phys. Chem.* **1985**, *89*, 5427.

(15) (a) De Menorval, L. C.; Fraissard, J. *P. Chem. Phys. Lett.* **1981**, *77*, 309. (b) Reineke, N.; Haul, R. *J. Phys. Chem.* **1984**, *88*, 1232–1238.

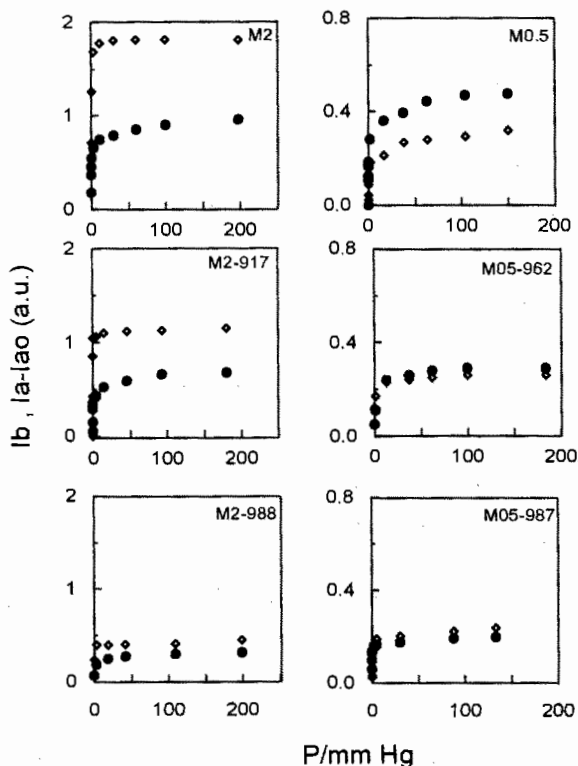


**Figure 4.** Evolution of Ia (open symbols) and Ib (full symbols) intensities versus hydrogen pressure in fresh and sintered M05 and M2 catalysts.

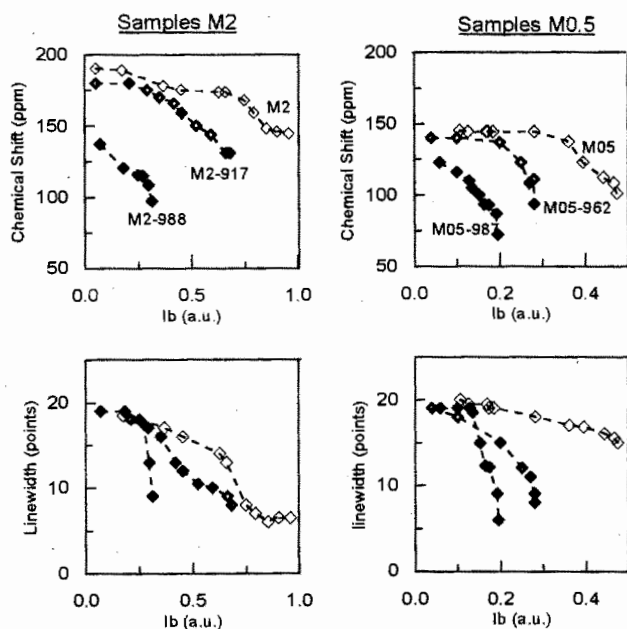


**Figure 5.** Plot of chemical shift  $\delta$  (ppm) and line width (ppm) versus line B intensity in M05 and M2 catalysts.

**High-Resolution Electron Microscopy Data.** Because of the contrast between the metal (Rh) and the support (Al<sub>2</sub>O<sub>3</sub>), the HREM technique has been used to follow the effect of the sintering temperature on metal dispersion. Figure 6 shows representative images of fresh and sintered samples, taken with the same magnification, in M2 and M05 catalysts. Detection of lattice fringes in particles of the more sintered samples has allowed the identification of metallic rhodium {111} planes.

As clearly shown by metal particle size distribution curves obtained for M2 and M05 catalysts (Figure 7), the increase of the sintering temperature produces the growth

of rhodium particles. The mean particle size changed from 17 Å in the starting M2 sample to 22 Å in M2-917 K and up to 69 Å in M2-988 K; in M05 sample, the mean particle size changed from 12 Å to 37 Å in M05-962 K and up to 46 Å in M05-988 K. In general, the metal sintering is accompanied by a progressive broadening of the particle size distribution. Likewise, sintering leads to well-faceted hexagonal faces in the rhodium particles. This kind of contrast in HREM images is consistent with truncated cubo-octahedral geometry.<sup>17</sup>

The HREM images also suggest differences in the homogeneity of metal dispersion in the M05 and M2 samples. Thus, the comparison of parts a-I and b-I of Figure 6 shows that regions with rather similar densities of metal particles can be observed in both catalysts. Because metal loading is 4 times larger in the case of the M2 catalyst, we should conclude that the rhodium distribution is less homogeneous in the M05 sample. Finally, the coverage of metal particles detected in the M05 catalyst is also noteworthy. An example is given in Figure 6b-III where rhodium particles appear decorated by a thin amorphous layer, probably consisting of alumina.

## Discussion

To correlate <sup>1</sup>H NMR spectral intensities with the amount of hydrogen adsorbed on the catalysts, intensity values, Ib + Ia - Ia<sub>0</sub>, deduced from NMR spectra were plotted versus volumetric adsorption data (Figure 8). In this expression, Ia<sub>0</sub> stands for the intensity of line A before adsorption. A good linear dependence passing through the origin is observed, demonstrating that all the hydrogen adsorbed on the catalyst is detected with <sup>1</sup>H NMR spectroscopy. The relationship obtained has been used in this work to calibrate the intensities of NMR lines.

From hydrogen adsorption data, metal dispersions were estimated (Table 1). In the case of NMR determinations, only the hydrogen adsorbed on metal particles (line B) was used, so metal dispersions obtained were always lower than those determined from volumetric techniques (Table 1). A HREM study was carried out to elucidate this point. In all cases, dispersions obtained with HREM were intermediate between those obtained with NMR and volumetric techniques (Figure 9). This effect is particularly noticeable in the case of the catalyst reduced at the lowest temperature. This effect could be due to the spill-over contribution to the total hydrogen adsorption. Two observations support this interpretation. First, the evolution with time of the O-D stretching region in the FTIR spectrum for the M2 catalysts reduced/evacuated at 723 K and further treated with D<sub>2</sub> (40 Torr) at 298 K (Figure 10) shows that, under experimental conditions similar to those applied in the volumetric studies, a hydrogen transfer from the metal to the support is produced. Similar observations have been reported elsewhere.<sup>18-20</sup> This point is here confirmed by NMR study of the samples; because the number of metal particles is much larger in the high-loaded catalysts (M2) and the metal dispersion does not dramatically change from M05 to M2 samples, the spill-over contribution, as deduced from the increase of line A intensity in the NMR spectra, is larger in the M2 catalyst. From these facts, we conclude that the amount of hydrogen

(17) Bernal, S.; Botana, F. J.; Calvino, J. J.; López-Cartes, C.; Pérez-Omil, J. A.; Rodríguez-Izquierdo, J. M. *Ultramicroscopy* **1998**, *72*, 135-164.

(18) Dalla Betta, R. A.; Boudart, M. *J. Chem. Soc., Faraday Trans.* **1976**, *72*, 1673.

(19) Cavanagh, R. R.; Yates, J. T., Jr. *J. Catal.* **1981**, *68*, 22-26.

(20) Fang, T. H.; Wey, J. P.; Neely, W. C.; Worley, S. D. *J. Phys. Chem.* **1993**, *97*, 5128-5131.

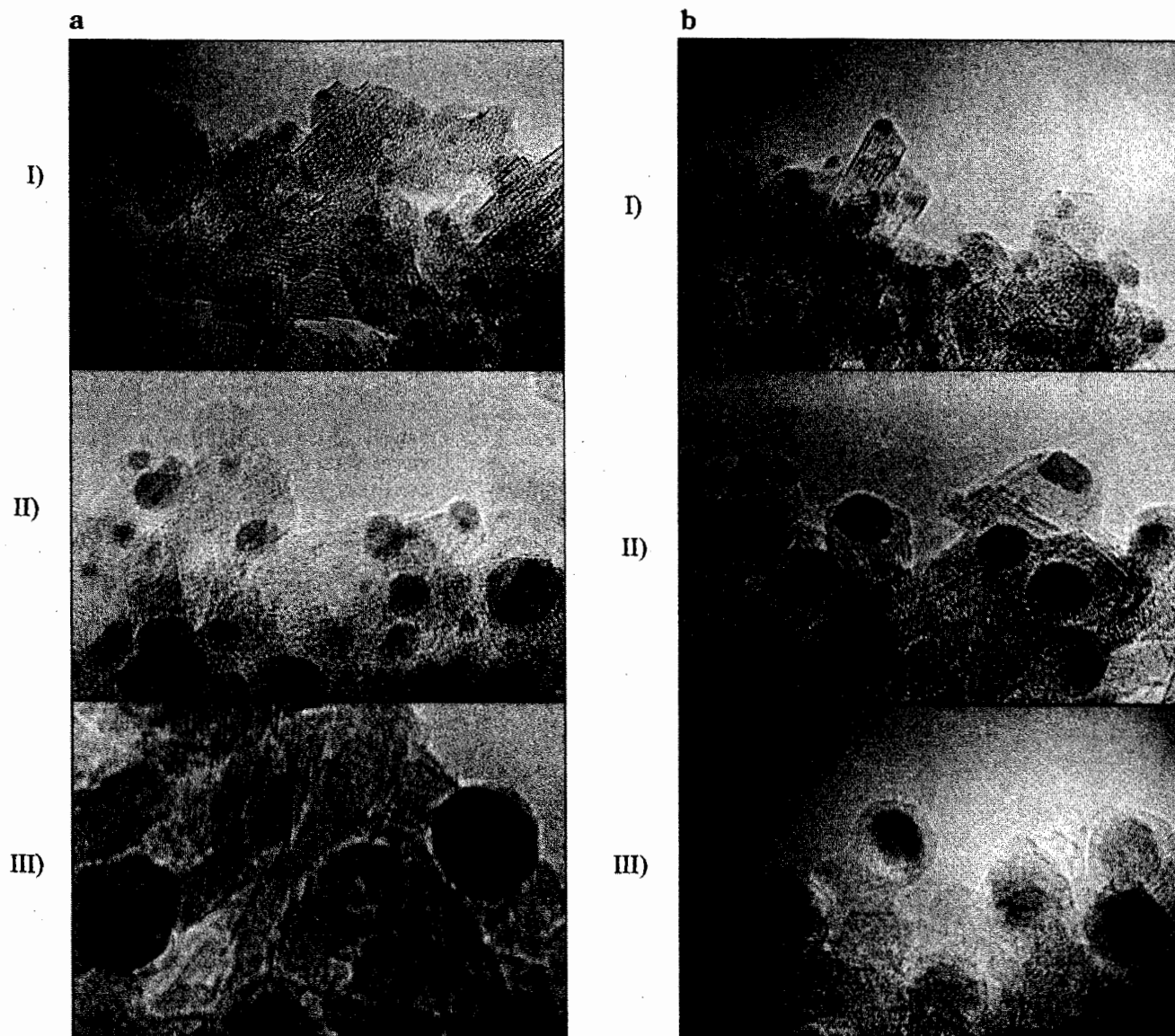


**Figure 6.** HREM micrographs of (a) M2 and (b) M05 catalysts submitted to increasing sintering temperatures: (I) starting sample; (II) catalysts reduced at 917 and 926 K, respectively; (III) catalysts sintered at 987 and 988 K. All images are displayed at the same magnification.

adsorbed on the metal is systematically overestimated by volumetric techniques.

Another reason that could explain high metal dispersion values deduced from volumetric data could be the presence of hydrogen adsorbed on Rh extremely dispersed on the alumina surface, undetectable by HREM ( $\varnothing < 10 \text{ \AA}$ ), displaying chemical shifts approximately 0, because of the lack of metal character. Hydrogen adsorption in these clusters would produce only an increment of line A in the NMR spectra. Rhodium atomically dispersed has been reported by Soria et al. in rhodium catalysts supported on  $\text{SrTiO}_3$ ,  $\text{TiO}_2$ , and  $\text{CeO}_2$  oxides, by means of the electron paramagnetic resonance technique.<sup>21</sup> In this case, dispersion values deduced from volumetric techniques should be again higher than those obtained with the HREM and NMR techniques.

Finally, metal dispersions determined from NMR (line B) are lower than those estimated by HREM. To explain these differences, it has been supposed that the amorphous coverage of metal particles formed during catalyst prepa-

ration could block part of the metal sites and reduce H/Rh values deduced from NMR spectroscopy. Evidence of metal covering with a thin layer of amorphous material, probably alumina, has been appreciated by means of the HREM technique in M05 catalysts. In M2 catalysts, this effect could also be present but it is difficult to evidence it by HREM. Actually, an estimation of the relative importance of the three mentioned effects in metal dispersion determination cannot be done.

From data obtained with the three techniques, it is possible to get information about the mean metal particle size. Whereas the HREM technique gives direct information on metal particle size, volumetric and NMR techniques require the application of the known expression

$$\phi = \frac{6M_{\text{Rh}}}{\rho_{\text{Rh}}\sigma_{\text{Rh}}N_{\text{a}}d}$$

that relates the mean particle diameter ( $\phi$ ) (nm) to the metal dispersion ( $d$ ). In this expression,  $\rho_{\text{Rh}}$  ( $\text{g/cm}^3$ ) is the density of the metal,  $\sigma_{\text{Rh}}$  is the surface covered by one exposed rhodium atom ( $\text{nm}^2/\text{atom}$ ),  $N_{\text{a}}$  is the Avogadro

(21) Soria, J.; Martinez Arias, A.; Coronado, J. M.; Conesa, J. C. *Top. Catal.* **2000**, *11/12*, 205.

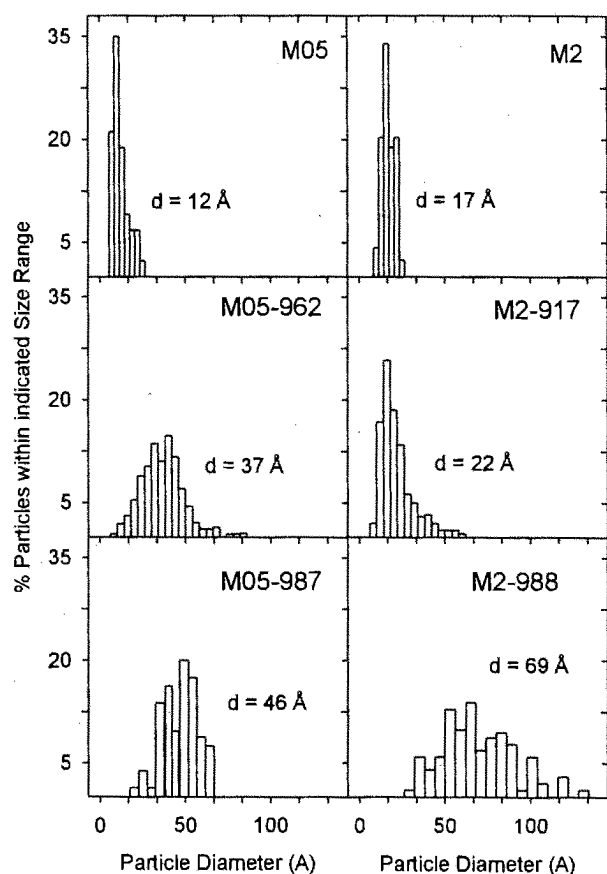


**Figure 7.** Particle size distribution as determined from the analysis of tens of HREM micrographs, in starting and sintered M05 and M2 catalysts.

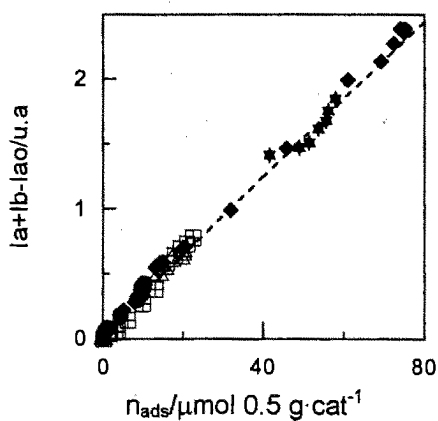


**Figure 8.** Plot of hydrogen uptakes deduced from the <sup>1</sup>H NMR spectra ( $I_b + I_a - I_{a_0}$ ) versus those obtained from volumetric measurements ( $n^{\sigma}$ ).  $I_{a_0}$  corresponds to the intensity of line A in the samples outgassed.

constant (atom/mol), and  $M_{Rh}$  is the rhodium atomic weight (g/mol). Metal particle sizes deduced with the three techniques are given in Table 2. To make the comparison of data deduced from HREM, NMR, and volumetry more reliable, mean metal particles sizes deduced from HREM histograms were calculated with  $\sum(n_i d_i) / \sum(n_i)$  and  $\sum(n_i d_i^3) / \sum(n_i d_i^2)$  expressions (columns a and b in Table 2). The last expression takes into account contributions of particles with different sizes to adsorption phenomena.

Metal particles sizes deduced from NMR are very close to those calculated with HREM but differ from those obtained with volumetric techniques. This fact shows the importance of differentiating adsorptions produced on the metal and the support and underlines difficulties in

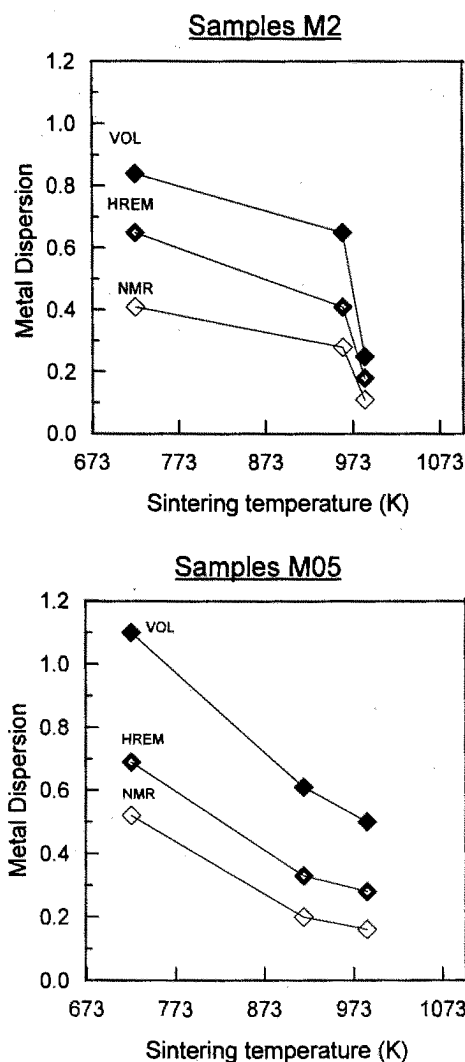


**Figure 9.** Metal dispersions, H/Rh, deduced from HREM, NMR, and volumetric data versus sintering temperature in M05 and M2 catalysts.

obtaining good values for metal particle size from volumetric adsorption data (see Table 2).

On the other hand, the position of <sup>1</sup>H NMR line B changes with the metal particle size. This effect was first studied by Kubo's and Denton's groups for very small particles, predicting a different behavior for metals with odd and even numbers of electrons.<sup>22,23</sup> Rh metal has an unpaired electron spin ( $4d^7$ ) in the atomic state; however, as the particle size increases, spins begin to pair approaching the metal band structure, making the absolute value of the chemical shift decrease. Chang et al.<sup>24</sup> have reported an important NMR shift for small metal particles,  $-200$  ppm, that decreases toward  $-125$  ppm when metal particle size increases up to  $60$  Å. This behavior is different in samples with even electron configurations, such as Pt ( $5d^8$ ), which displays a low paramagnetism in small metal particles. For bigger particles, the NMR line B shift does not change significantly. On the other hand, hydrogen adsorption on more energetic adsorption sites produces  $\delta_B$  values higher than those seen for adsorption on weaker sites;<sup>25</sup> from this fact, a comparison of NMR shifts

(22) Kubo, R. *J. Phys. Soc. Jpn.* **1962**, *17*, 975.

(23) Denton, R.; Muhlschlegel, B.; Scalapio, D. *Phys. Rev. Lett.* **1971**, *26*, 707.

(24) Chang, T.-H.; Cheng, C. P.; Yeh, C.-T. *J. Catal.* **1992**, *138*, 457-462.

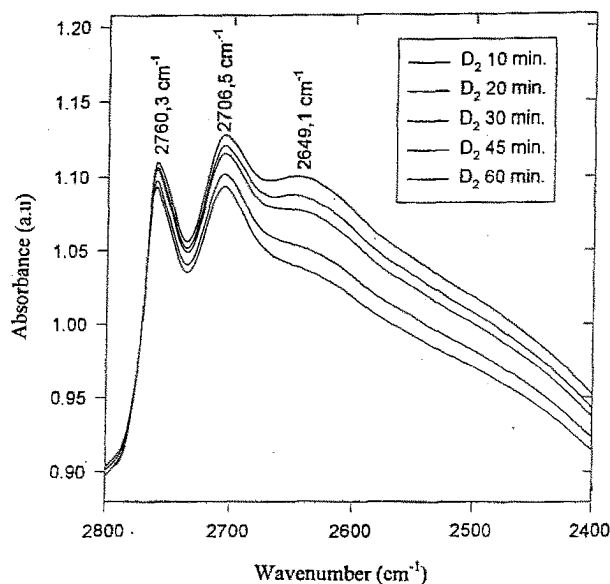


**Figure 10.** Spill-over phenomena as revealed by the evolution with time of the O–D stretching region in the FTIR spectra of M2 catalysts reduced/evacuated at 723 K (1 h) and further treated at 298 K (1 h) with 40 Torr of D<sub>2</sub>. The spectrum corresponding to the reduced/evacuated sample, prior to the D<sub>2</sub> treatment, was used as a reference.

**Table 2. Mean Metal Particle Size Deduced from Volumetry, HREM, and NMR Data<sup>a</sup>**

sample	volumetric size (nm)	HREM size (nm)		NMR size (nm)	Knight shift (ppm)
		(a)	(b)		
M2	1.0	1.7	1.8	2.2	-188
M2-917	1.3	2.2	3.2	3.4	-180
M2-988	3.6	6.9	8.2	8.2	-137
M05	<1	1.2	1.6	1.7	-145
M05-962	1.5	3.7	4.5	4.8	-140
M05-988	3.2	4.6	5.1	5.7	-123

<sup>a</sup> HREM values were calculated from histograms using  $\sum(n_i d_i) / \sum(n_i)$  (a) and  $\sum(n_i d_i^3) / \sum(n_i d_i^2)$  (b) expressions (see text). In the last column, the NMR shifts of line B,  $\delta_B$ , measured at low H<sub>2</sub> pressures (5 Torr) are also included.

measured on samples with different metal particle sizes must be done at low pressures (<10 Torr), when the occupation of the second type of sites has not been produced and hydrogen mobility is low.

In two Rh/Al<sub>2</sub>O<sub>3</sub> catalysts analyzed, line B shifts measured at 5 Torr decrease with metal particle size (Figure 11) in agreement with previous works. However, in M05 samples, where metal particle sizes are smaller than those in M2 catalysts, shifts are lower. A decrease of this parameter could be produced by poisoning of more energetic metal sites. As metal support interactions are unlikely in Rh/Al<sub>2</sub>O<sub>3</sub> catalysts, we think, in agreement with HREM observations, that the observed small values are mainly due to poisoning of stronger metal sites by amorphous Al<sub>2</sub>O<sub>3</sub> species deposited during catalyst preparation. Adsorption on the remaining metal sites will produce the lower NMR shifts observed in the <sup>1</sup>H NMR spectra of M05 catalysts. The presence of metal coverage impedes the generalized use of the  $\delta_B$  parameter for metal particle characterization.

Finally, it is interesting to analyze the calorimetric curves recorded for increasing amounts of adsorbed hydrogen,  $n^\circ$ . The resolution of two types of adsorption in the calorimetric curves must be ascribed to the existence

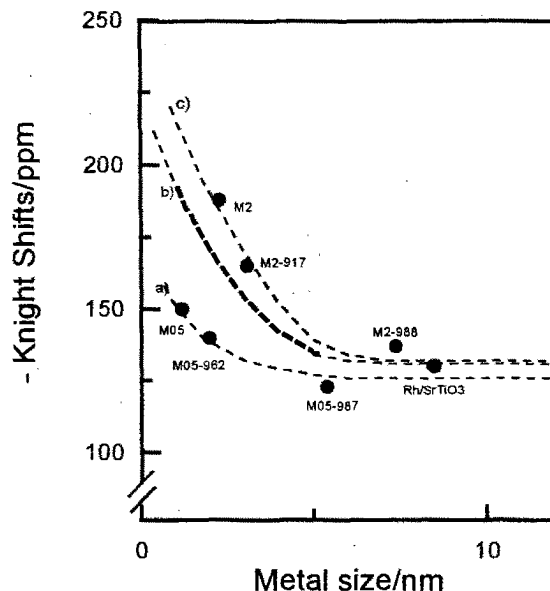


**Figure 11.** Plot of  $\delta_B$  shifts versus particle size in (curve a) M05 and (curve c) M2 catalysts submitted to increasing sintering temperatures. Plotted values correspond to spectra recorded at 5 Torr. Curve b correspond to data of ref 22 included as reference.

of two adsorption sites identified by NMR on metal particles. On the other hand, the analysis of the differential calorimetric isotherms shows that  $q^{st,\sigma}$  values measured at low metal coverages decrease with metal sintering. However, in the case of M05 the evolution of  $q^{st,\sigma}$  with metal sintering is much lower than in M2 catalysts, again supporting HREM observations concerning blocking of the most energetic metal sites by amorphous Al<sub>2</sub>O<sub>3</sub> species. In this case, adsorption of hydrogen on weaker sites explains the lower calorimetric  $q^{st,\sigma}$  and NMR shift  $\delta_B$  values measured.

## Conclusions

The simultaneous use of HREM, NMR, and volumetric techniques allowed us to study the metal sintering produced during the treatment of Rh/Al<sub>2</sub>O<sub>3</sub> catalysts at increasing temperatures. Metal dispersions deduced from the NMR shifted line B are considerably lower than those deduced from volumetric techniques. The hydrogen spill-over or the hydrogen adsorption on Al<sub>2</sub>O<sub>3</sub> located near metal particles has been invoked to explain the observed increment of the nonshifted line A, that produces the observed discrepancies between NMR and volumetric data. Hydrogen adsorption on very small particles, undetectable by HREM, could also produce the increment of the NMR line A detected. Metal particle sizes deduced from the intensity of NMR line B agree well with those deduced from HREM, when metal particle size distributions was taken into account.

In the case of M2 catalysts, the dependence of the shift of line B with metal particle sizes agrees with the prediction of Kubo et al. and Denton et al. However, in the case of M05 catalysts the partial coverage of metal particles with amorphous Al<sub>2</sub>O<sub>3</sub> decreased the NMR shift measured at low  $P_{H_2}$ , making the utilization of this parameter unreliable in the case of supported metal particles analyzed.

**Acknowledgment.** Financial support from CICYT (Spain) under Project MAT98-0971 is acknowledged. C.F. is grateful to Volkswagen-Audi-CSIC for the grant received.